Far Cortical Locking Can Improve Healing of Fractures Stabilized with Locking Plates

By Michael Bottlang, PhD, Maren Lesser, DVM, Julia Koerber, MS, Josef Doornink, MS, Brigitte von Rechenberg, DVM, ECVS, Peter Augat, PhD, Daniel C. Fitzpatrick, MD, Steven M. Madey, MD, and J. Lawrence Marsh, MD

Investigation performed at the Legacy Biomechanics Laboratory, Portland, Oregon; the University of Zürich, Zürich, Switzerland; and the Institute of Biomechanics, Murnau, Germany

Background: Locked bridge plating relies on secondary bone healing, which requires interfragmentary motion for callus formation. This study evaluated healing of fractures stabilized with a locked plating construct and a far cortical locking construct, which is a modified locked plating approach that promotes interfragmentary motion. The study tested whether far cortical locking constructs can improve fracture-healing compared with standard locked plating constructs.

Methods: In an established ovine tibial osteotomy model with a 3-mm gap size, twelve osteotomies were randomly stabilized with locked plating or far cortical locking constructs applied medially. The far cortical locking constructs were designed to provide 84% lower stiffness than the locked plating constructs and permitted nearly parallel gap motion. Fracture-healing was monitored on weekly radiographs. After the animals were killed at week 9, healed tibiae were analyzed by computed tomography, mechanical testing in torsion, and histological examination.

Results: Callus on weekly radiographs was greater in the far cortical locking constructs than in the locked plating constructs. At week 9, the far cortical locking group had a 36% greater callus volume ($p = 0.03$) and a 44% higher bone mineral content ($p = 0.013$) than the locked plating group. Callus in the locked plating specimens was asymmetric, having 49% less bone mineral content in the medial callus than in the lateral callus ($p = 0.003$). In far cortical locking specimens, medial and lateral callus had similar bone mineral content ($p = 0.91$). The far cortical locking specimens healed to be 54% stronger in torsion ($p = 0.023$) and sustained 156% greater energy to failure in torsion ($p < 0.001$) than locked plating specimens. Histologically, three of six locked plating specimens had deficient bridging across the medial cortex, while all remaining cortices had bridged.

Conclusions: Inconsistent and asymmetric callus formation with locked plating constructs is likely due to their high stiffness and asymmetric gap closure. By providing flexible fixation and nearly parallel interfragmentary motion, far cortical locking constructs form more callus and heal to be stronger in torsion than locked plating constructs.

Clinical Relevance: Far cortical locking fixation may be advisable for stiffness reduction of locked bridge plating constructs to improve fracture-healing.

The benefits of locked plating, including improved fixation strength in osteoporotic bone[1-3] and the ability to provide a more biologically friendly fixation construct[4,5], have led to the rapid adoption of this technology. Because interfragmentary compression is typically not sought or obtained, biological fixation of comminuted fractures with locking plates relies on secondary fracture-healing by callus formation[6,7]. However, controversy persists with regard to whether locked plating constructs provide a proper mechanical environment to reliably promote secondary bone healing by callus formation[1,2,8,9].

Secondary bone healing is stimulated by interfragmentary motion in the millimeter range[10,11] and is enhanced by active or passive dynamization[12,13]. Conversely, secondary bone healing can be suppressed by rigid fixation aimed at preventing interfragmentary motion[14]. Locked plating constructs have been described as internal fixators, capable of providing relative stability while allowing controlled micromotion at the fracture

Disclosure: In support of their research for or preparation of this work, one or more of the authors received, in any one year, outside funding or grants in excess of $10,000 from the National Institutes of Health (National Institute of Arthritis and Musculoskeletal and Skin Diseases R21 AR053611) and Zimmer. In addition, one or more of the authors or a member of his or her immediate family received, in any one year, payments or other benefits in excess of $10,000 (Zimmer) and less than $10,000 (Stryker) or a commitment or agreement to provide such benefits from these commercial entities.

zone to promote secondary bone healing[4,5,15]. However, locking constructs are several times stiffer than external fixators because of their close proximity to the bone[16]. They are reported to be as stiff as conventional plating constructs designed to induce primary bone healing[1]. Therefore, locked bridge plating constructs may be too stiff to promote callus formation reliably[2,8,9]. To date, no in vivo study of fracture-healing has been published to document callus formation associated with locked plating constructs.

To address this stiffness concern, a modified locked plating technology, termed *far cortical locking*, capable of reducing the stiffness of a locked plating construct while retaining its strength, has been introduced recently[17]. In far cortical locking constructs, locking screws with a reduced midshaft diameter provide unicortical fixation in the far cortex of a diaphysis without being rigidly fixed in the near cortex underlying the plate. The far cortical locking screws decrease the stiffness of the plating construct by acting as elastic cantilever beams similar to half-pins of an external fixator.

The present study evaluated healing of fractures stabilized with a locked plating construct and a far cortical locking construct in an ovine transverse osteotomy model. By comparing fracture-healing between the locked plating and far cortical locking constructs, this study examines the effect of locked construct stiffness on fracture-healing. We hypothesized that a stiffness-reduced far cortical locking construct can substantially improve fracture-healing compared with a standard locked plating construct.

Materials and Methods

With use of an established fracture-healing model[18], standard tibial transverse osteotomies with a 3-mm gap width in twelve sheep were randomly assigned for stabilization with locked plating constructs or far cortical locking constructs. Progression of fracture-healing was monitored radiographically by weekly assessment of periosteal callus formation. After the animals were killed at nine weeks after surgery, the implants were removed and callus volume and density were measured with computed tomography. The mechanical strength of the healed tibiae was assessed by torsion testing to failure. Finally, callus formation and bridging were analyzed on histological cross sections.

Plating Constructs

Generic locked plating implants were designed to closely replicate standard 4.5-mm osteosynthesis plates and screws that are commercially available from several manufacturers, while accounting for the anatomic contour of the ovine tibia (Fig. 1, *A*). All implants were professionally manufactured from surgical grade titanium alloy (Ti-6Al-4V). The plates were 117 mm long, 17 mm wide, and 5.6 mm thick, and they had a longitudinal curvature with a 750-mm radius. Six threaded screw-holes were arranged in a staggered pattern to enhance torsional stability. Self-tapping locking screws had a 4.5-mm-diameter cortical thread. The only difference between locked plating and far cortical locking constructs was the far cortical locking screw design, which had a smooth screw shaft with a 3-mm diameter to bypass the near cortex (Fig. 1, *B*). The resulting unicortical fixation of far cortical locking screws in the far cortex allows for elastic cantilever bending of the screw shaft within a controlled motion envelope in the near cortex. This elastic fixation with far cortical locking screws induces principally parallel interfragmentary motion under axial load (Fig. 1, *C*). At higher axial loads, contact between the far cortical locking screw shaft and the near cortex provides additional support and prevents the far cortical locking shaft bending beyond the elastic range. Analogous to external fixator pins, far cortical locking screws derive their low stiffness by elastic bending of the screw shafts (Fig. 1, *D*). A detailed description and formal biomechanical evaluation of far cortical locking constructs has been published[17].

Construct stiffness was characterized by bench testing of three locked plating and three far cortical locking constructs applied to bridge 3-mm-gap osteotomies in six ovine cadaveric tibiae. A full description of this stiffness characterization is provided in the Appendix. Locked plating constructs had a mean stiffness (and standard deviation) of 3922 ± 474 N/mm. Up to an axial load of 400 N, far cortical locking constructs had a mean stiffness of 628 ± 81 N/mm (84% lower stiffness than locked plating constructs) and exhibited nearly parallel motion at the osteotomy gap. For loads of >400 N, the mean stiffness of far cortical locking constructs increased to 2672 ± 594 N/mm because of additional structural support provided by contact between the near cortex and the far cortical locking screw shafts.

Animal Model and Surgical Procedure

An established ovine tibial osteotomy model was selected for this study as it represents the most prevalent large animal model for the evaluation of fracture-healing[18,19]. The protocol conformed to the National Institutes of Health Guide for the Care and Use of Laboratory Animals and was approved by the pertinent animal care committees. Twelve skeletally mature female Swiss Alpine sheep, with an average age of 2.5 ± 0.8 years and an average weight of 61 ± 9 kg, were randomly divided into a locked plating group and far cortical locking group. The sample size of six sheep per group was determined a priori to be sufficient in detecting a 20% change in torsional strength with 80% confidence, on the basis of the standard deviation of torsional strength results reported in a prior study[20]. With the sheep under general anesthesia with isoflurane, the right hind leg was sterilely draped and an approximately 8-cm-long medial incision was made over the tibia. To control the osteotomy gap size after plate application, six screw-holes for plate fixation were drilled in the intact tibia with a drill template. The periosteum was incised around the designated osteotomy plane and retracted 2 mm to minimize irritation of the periosteum by the oscillating saw[21]. A custom saw guide was affixed to the screw-holes to perform a transverse osteotomy centered on the tibial diaphysis with use of a 0.6-mm-thick saw blade and constant irrigation with 0.9% NaCl solution. Osteotomies were

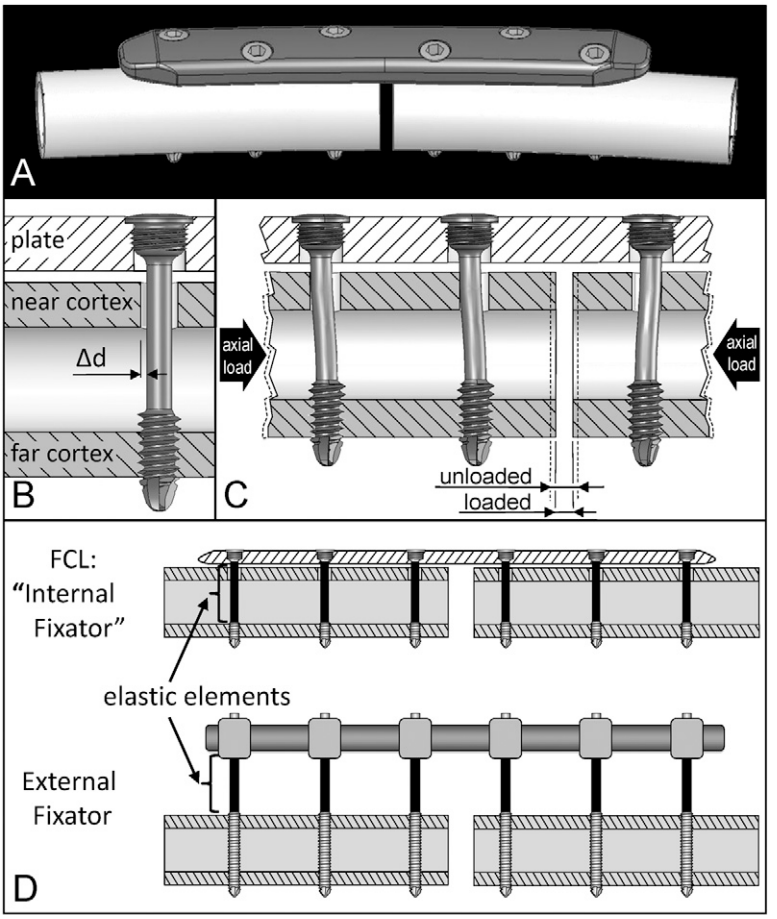

Fig. 1

Fixation constructs. *A:* Locking plate (LP) with anatomic curvature of the ovine tibia. *B:* Far cortical locking (FCL) screw for unicortical fixation in the far cortex, enabling elastic flexion of the screw shaft within the motion envelope (Δ*d*) in the near cortex. *C:* Nearly parallel interfragmentary motion provided by far cortical locking screws under axial loading. *D:* Mechanically, far cortical locking constructs derive elastic fixation by cantilever bending of far cortical locking screw shafts similar to an external fixator that derives elasticity from fixation pin flexion.

stabilized with locking plates applied with three locking screws proximal and distal to the osteotomy. The distance between the proximal and distal screw-holes in the locking plate was 2.4 mm greater than in the drill template. Combined with the 0.6-mm saw blade cut, the locking plate application therefore yielded a 3-mm osteotomy gap. For periosteum-sparing biological fixation, all plates were applied at a 1-mm elevation with use of temporary spacers[4]. Plate elevation and osteotomy gap size were verified on postoperative radiographs. The limb was protected by a cast applied over a soft padding layer, and the sheep were allowed to walk in a restricted area immediately after surgery. As a routine prophylactic measure to avoid tibial fracture of the operatively treated limb[13,19,22,23], the sheep remained in a protective harness for three weeks after surgery and the cast was changed regularly. This loosely applied harness and the cast allowed full load-bearing while standing, and the sheep were able to walk freely within their stall[23]. However, the protective harness suspended the animals during sleep to prevent peak loads during standing or sudden bolting from a lying position. Nine weeks after surgery, the sheep were killed and fracture-healing was evaluated by radiography, mechanical testing, and histological analysis.

Radiography

Radiographs were made immediately postoperatively and at weekly intervals, starting at postoperative week 3. The osteotomy gap width was measured on the radiographs to document the accuracy of fixation and changes thereof over time. Weekly follow-up radiographs were analyzed to assess the progression of callus formation, which represents the principal hallmark of secondary bone healing. The projected areas of periosteal callus at the anterior, lateral, and posterior aspects were quantified on lateral and anteroposterior radiographs, with use of validated custom software developed to objectively quantify periosteal

TABLE I Comparison of Outcome Parameters Between Locked Plating and Far Cortical Locking Groups

	Locked Plating Group*	Far Cortical Locking Group*	Difference *(%)*	P Value
Sheep				
Weight *(kg)*	63 (11)	59 (6)	6	0.45
Age *(mo)*	30.8 (13.2)	28.0 (6.2)	9	0.64
Osteotomy gap width *(mm)*				
Postop.	3.0 (0.2)	3.1 (0.2)	3	0.37
Week 4	3.2 (0.1)	3.1 (0.5)	–3	0.41
Callus volume *(mm^3)*				
Medial	1584 (325)	3016 (972)	90	0.006
Lateral	2790 (628)	2934 (730)	5	0.72
Total	4374 (841)	5950 (1300)	36	0.03
Bone mineral content *(mg hydroxyapatite)*				
Medial	971 (163)	2103 (563)	117	0.001
Lateral	1918 (485)	2063 (611)	8	0.66
Total	2889 (598)	4166 (820)	44	0.013
Mechanical properties				
Torsional stiffness *(Nm/°)*	4.4 (1.4)	5.1 (0.8)	16	0.36
Torsional strength *(Nm)*	28 (12)	43 (6)	54	0.023
Torsional energy to failure *(Nm°)*	110 (54)	282 (55)	156	<0.001

*The values are given as the mean, with the standard deviation in parentheses.

callus size[24]. No periosteal callus could be assessed at the near (medial) cortex because of plate interference.

After specimen harvest and implant removal at week 9, the total volume and bone mineral content of callus per specimen were determined by quantitative computed tomography scanning of the excised tibiae in accordance with an established protocol[25]. Scanning was performed at a slice thickness of 0.4 mm and an in-plane voxel size of 0.35 mm (LightSpeed VCT; GE Healthcare, Waukesha, Wisconsin). The scanner was calibrated with a hydroxyapatite phantom for transformation of Hounsfield units (H) into bone mineral density. Callus volume was rendered in Amira visualization software (Visage Imaging, San Diego, California), with use of consistent thresholds of 80 H and 1600 H to differentiate callus from soft tissue and cortical bone, respectively. As a summary index for callus proliferation, bone mineral content was calculated as the product of callus volume and bone mineral density.

Mechanical Testing

The stiffness and strength, as well as the torsional displacement and the energy to failure, of the healed tibiae were tested under torsional loading to failure. The proximal and distal ends of the tibiae were rigidly embedded with use of bone cement in mounting fixtures that were separated by 170 mm and aligned with the tibial shaft axis. Tibiae were suspended in a materials testing system (model 8874; Instron, High Wycombe, United Kingdom). To minimize alignment artifacts, the proximal fixture was attached to a universal joint that permitted rotations around anteroposterior and mediolateral axes but prevented rotation around the diaphyseal axis[10]. The distal fixture was mounted on an x-y table to minimize alignment artifacts. Rotation around the tibial shaft axis was applied at a rate of 10° per minute under an axial preload of 20 N. Torsional stiffness was calculated from the linear slope of the torsion versus rotation curve between 2 and 5 Nm of torsion. It represented the torsional moment required to induce 1° of rotation around the tibial shaft axis. Torsional strength was defined as the highest torsional moment recorded during the test to failure. Energy to failure was calculated by integrating the area under the torsion versus rotation curve up to the peak torsional moment at which fracture occurred.

Histological Analysis

Callus specimens were fixed in 4% phosphate-buffered paraformaldehyde, dehydrated in ethanol, and embedded in methylmethacrylate for standard undecalcified histological analysis.

One longitudinal slice was harvested from the midsagittal plane of each callus specimen, ground to a 300-μm thickness, and surface stained with toluidine blue. Each slice was imaged under bright field microscopy, and the digital image was processed for visualization of callus differentiation and osteotomy gap bridging.

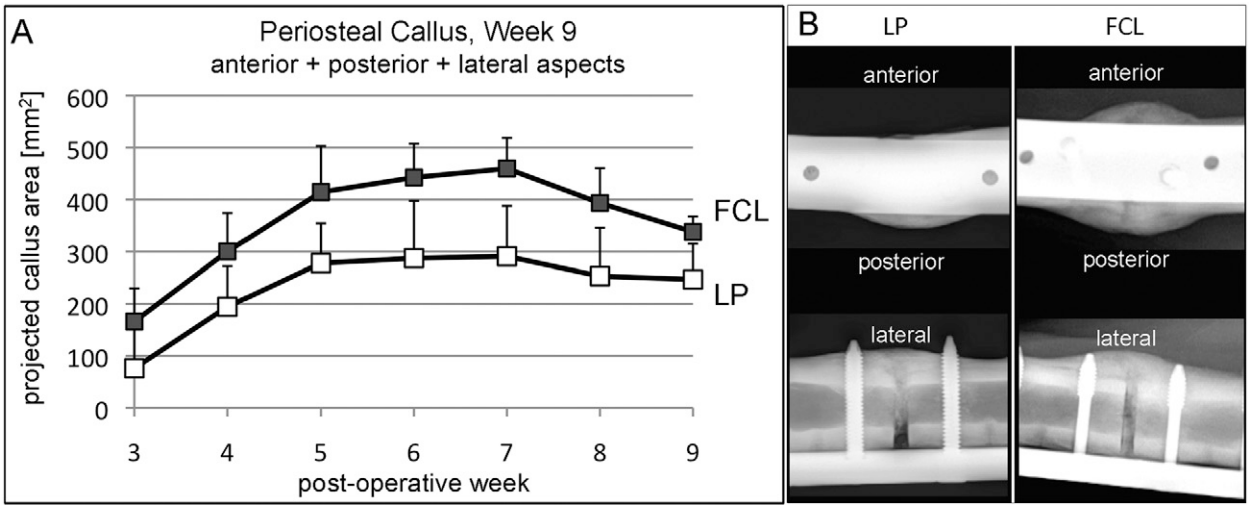

Fig. 2

Progression of periosteal callus formation. *A:* The far cortical locking (FCL) group formed significantly more callus (mean and standard deviation) than the locked plating (LP) group ($p = 0.004$). *B:* Callus projections at the anterior, posterior, and lateral aspects representative for far cortical locking and locked plating specimens at week 9 after surgery.

Statistical Analysis

All data are reported as the mean and the standard deviation. Statistical differences between the locked plating and far cortical locking groups were tested with use of two-tailed, unpaired Student t tests at a level of significance of $\alpha = 0.05$. The overall statistical difference in periosteal callus size between locked plating and far cortical locking groups from weekly radiographs was determined with repeated-measures analysis of variance. Paired testing was used to analyze differences in volume and bone mineral content between the medial half of the callus (near callus) and lateral half of the callus (far callus).

Source of Funding

Financial support for this study was provided by the Zimmer Corporation and by the National Institutes of Health (National Institute of Arthritis and Musculoskeletal and Skin Diseases grant R21 AR053611).

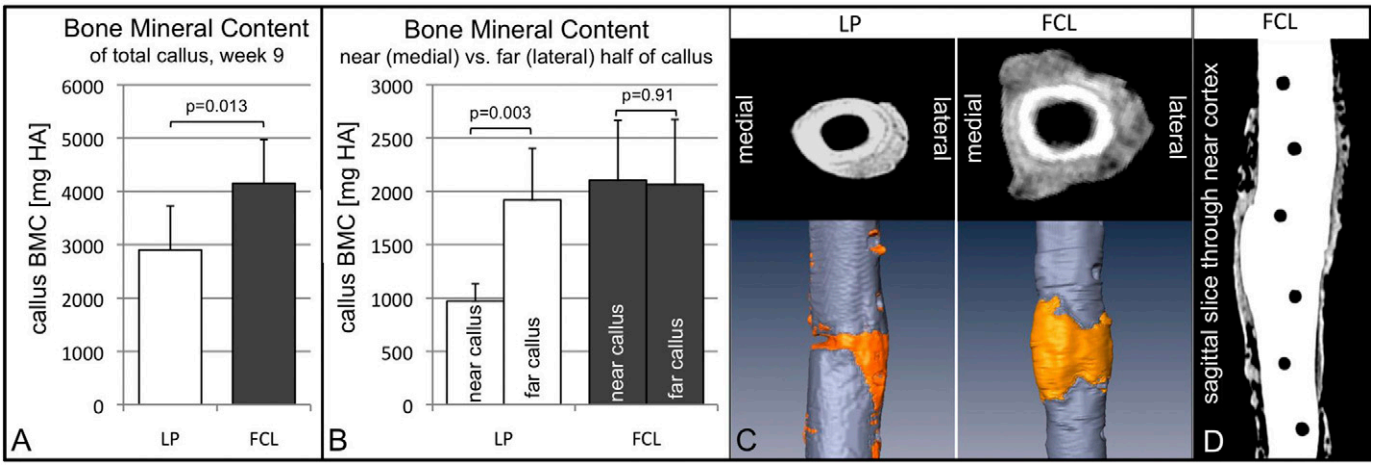

Fig. 3

Periosteal callus rendering from quantitative computed tomography data at week 9. *A:* Bone mineral content (BMC, mean and standard deviation in mg hydroxyapatite) in the far cortical locking (FCL) group was 43% greater than in the locked plating (LP) group. *B:* Far cortical locking constructs yielded symmetric callus formation, evident by equal bone mineral content in the medial half of the callus (near callus) and lateral half of the callus (far callus). Locked plating constructs had an asymmetric bone mineral content distribution, with 49% less bone mineral density in the near callus. *C:* Transverse slices adjacent to the osteotomy gap as well as callus volume rendered from computed tomography scans illustrate that callus formation was asymmetric in locked plating constructs, but extended from the far to the near cortex aspects in far cortical locking constructs, as reflected by the medial imprint of the plate. *D:* Parasagittal quantitative computed tomography slice extracted through the near cortex demonstrates that the far cortical locking screw-holes maintained clearly defined and circular boundaries.

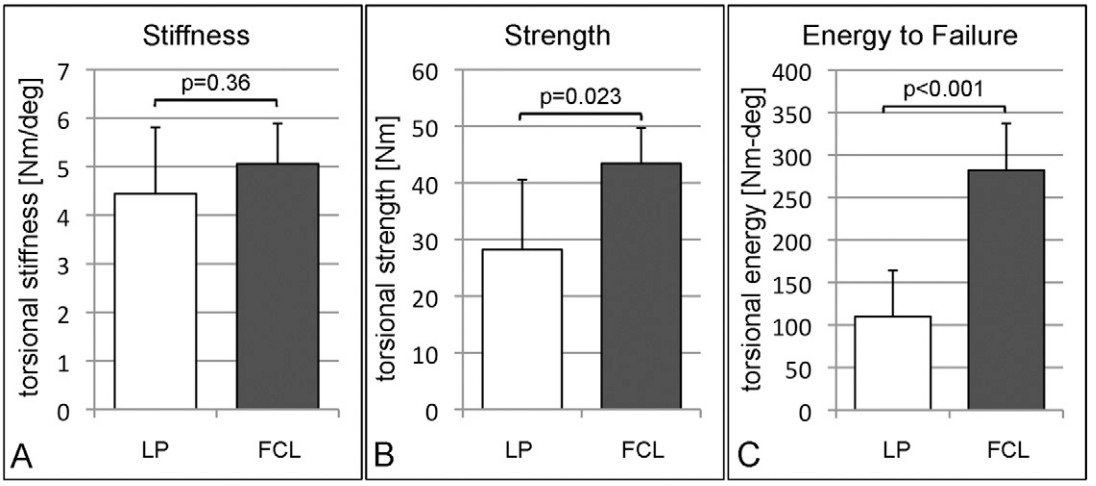

Fig. 4

Torsion test results after tibial harvest and implant removal at postoperative week 9 (mean and standard deviation). Compared with the locked plating (LP) group, tibiae in the far cortical locking (FCL) group were not significantly stiffer (A), but they healed to be 54% stronger (B), and they sustained 156% more energy before fracturing (C).

Results

All sheep tolerated the experimental procedure without complications, were able to walk on postoperative day 1, and retained stable fixation of the tibial osteotomy until they were killed at week 9. Immediately postoperatively, no significant difference was detected in the osteotomy gap width between the locked plating group (3.0 ± 0.2 mm) and the far cortical locking group (3.1 ± 0.2 mm; p = 0.37) (Table I). By postoperative week 4, gap width in the locked plating group had increased to 3.2 ± 0.1 mm (p = 0.03) and was unchanged at 3.1 ± 0.5 mm in the far cortical locking group (p = 0.8). Week 4 was the latest time point at which the gap width could be consistently measured on all radiographs before progressive healing obstructed visibility.

Radiographic Assessment of Callus

Callus progression on weekly radiographs demonstrated that the combined projected callus area at the anterior, posterior, and lateral aspects of the tibia was significantly greater in the far cortical locking group than in the locked plating group (p = 0.004) (Fig. 2). Periosteal callus increased continuously up to week 7, at which time the peak callus area in the far cortical locking group (460 ± 59 mm^2) was 58% greater than in the locked plating group (291 ± 97 mm^2; p = 0.005). At week 9, periosteal callus remained 37% greater in the far cortical locking group (338 ± 29 mm^2) than in the locked plating group (247 ± 68 mm^2; p = 0.01).

Volumetric rendering of callus from quantitative computed tomography data at week 9 yielded a 36% greater callus volume in the far cortical locking group compared with the locked plating group (p = 0.03) (Table I). The bone mineral content was 44% greater in the far cortical locking constructs than in the locked plating constructs (p = 0.013) (Fig. 3, *A*). In far cortical locking constructs, the medial half of the callus, termed *near callus,* had the same bone mineral content as the far callus (p = 0.91) (Fig. 3, *B*). In locked plating constructs, the near callus had 49% less bone mineral content than the far callus (p = 0.003). Accordingly, the near callus in the far cortical locking group had 90% greater volume (p = 0.006) and 117% higher bone mineral content (p = 0.001) compared with the locked plating group (Table I). Transverse quantitative computed tomography slices extracted adjacent to the osteotomy gap confirmed this asymmetric callus formation in locked plating constructs with deficient callus toward the near cortex (Fig. 3, *C*). Callus formation in far cortical locking constructs extended nearly symmetrically from the far cortex to the near cortex aspects of the osteotomy gap. Parasagittal quantitative computed tomography slices extracted through the near cortex demonstrated that far cortical locking screw-holes maintained clearly defined boundaries without apparent osteolysis or oval expansion (Fig. 3, *D*).

Mechanical Testing

Healed tibiae in the far cortical locking group were 16% stiffer in torsion than those in the locked plating group (Fig. 4, *A;* Table I), but this difference was not significant (p = 0.36). Testing to failure in torsion demonstrated that tibiae in the far cortical locking group healed to be 54% stronger (p = 0.023) than in the locked plating group (Fig. 4, *B*). Failure occurred at a 46% larger torsional displacement in the far cortical locking group (11.0° ± 1.0°) than in the locked plating group (7.5° ± 1.8°; p = 0.002). Compared with the locked plating group, the far cortical locking group absorbed 156% greater energy to failure (p < 0.001) (Fig. 4, *C*).

Histological Analysis

Histological sections showed that three of six locked plating specimens had deficient bridging at the near cortex with little or no new bone formation at the osteotomy gap adjacent to the plate (Fig. 5). In contrast, all six far cortical locking specimens

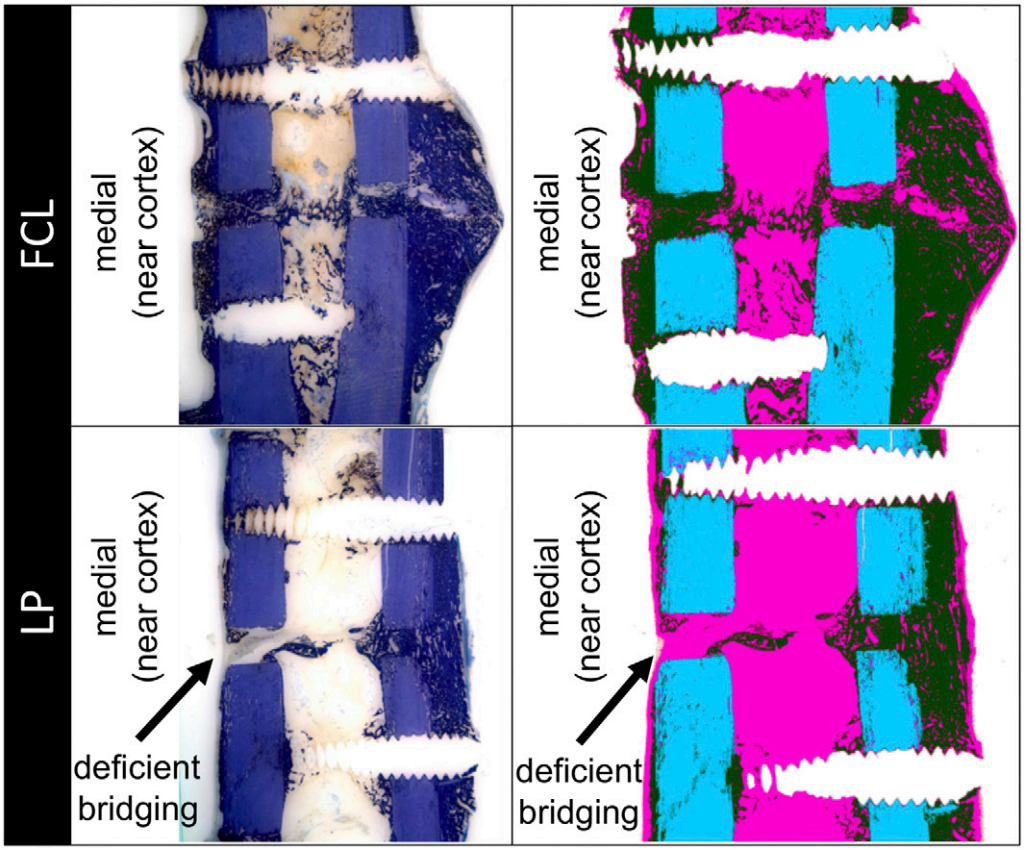

Fig. 5

Typical histological appearance of healing in the far cortical locking (FCL) and locked plating (LP) groups, shown with toluidine blue stain and after image processing for callus differentiation (green = callus, blue = cortex, and pink = fibrous tissue). Three of six locked plating specimens had deficient bridging at the near cortex, while all other near and far cortices had bridged.

showed complete bridging at the near cortex. All specimens in the locked plating and far cortical locking groups had bridged at the far cortex.

Discussion

This study suggests that construct stiffness and the resulting interfragmentary motion play a critical role in the healing of fractures stabilized with locked bridge plating constructs. The locked constructs with high stiffness suppressed interfragmentary motion to a level that inhibited callus promotion at the cortex underlying the plate. In the locked plating group, interfragmentary motion relied on plate bending, which resulted in asymmetric fracture site motion and callus formation. By applying cyclic plate bending in an ovine tibial osteotomy model, Cheal et al. similarly found that callus formation was smallest at the cortex adjacent to the plate, where interfragmentary motion was minimal[26]. Clinically, deficient callus formation near the plate may be difficult to detect radiographically as the plate often obscures visibility.

The relatively deficient callus formation in the locked plating group lends further support to the anecdotal concern that locked bridge plating constructs may be too stiff to promote secondary bone healing optimally[1,2,6,9]. This concern has led to the recommendation to increase the bridging span by omitting screw-holes adjacent to the fracture zone[5,27]. However, the reported efficacy in stiffness reduction is inconsistent. Stoffel et al. reported that increasing the plate span by omitting one screw-hole on either side of the fracture made a locked plating construct almost twice as flexible in compression and torsion[27]. In contrast, Field et al. reported that omitting two screws above and below the fracture had no significant effect on either bending or torsional stiffness of a conventional plate construct in a comparable bridge plating configuration[28].

The far cortical locking constructs of this study exhibited three characteristic factors that may promote secondary bone healing with locking plates: stiffness reduction, nearly parallel interfragmentary motion, and biphasic stiffness. As described in the Appendix, the stiffness reduction of the far cortical locking constructs relative to the locked plating constructs was more than sixfold and may have contributed to the formation of a larger callus with a higher bone mineral content in the far cortical locking group. The nearly parallel interfragmentary motion in the far cortical locking constructs is likely responsible for the callus formation at all aspects of the tibial oste-

otomy, yielding a comparable callus volume and bone mineral content at the near and far cortices. The biphasic stiffness of far cortical locking constructs allowed for progressive stabilization at elevated load levels because of additional support of the far cortical locking screws at the near cortex. This ability of far cortical locking constructs to bear elevated loads by screw support in the near and far cortices may be important in preventing fixation failure. This biphasic stiffness profile is comparable with the nonlinear behavior of Ilizarov fixators that become progressively stiffer with an increase in load[29].

Improved fracture-healing provided by flexible far cortical locking constructs is consistent with the results of previous in vivo studies that have evaluated less rigid plating[30-32]. Axially sliding plates yielded 24% stronger healing ($p < 0.05$) and a 25% higher energy to failure ($p < 0.05$) compared with rigid plating constructs in an ovine metatarsal osteotomy model[31]. Plates that had elastic inserts to permit axial flexibility yielded superior healing compared with standard compression plates in a canine femoral osteotomy model[30]. Finally, titanium plates yielded 33% stronger healing than geometrically identical yet stiffer stainless steel plates in an ovine femoral osteotomy model, but the difference did not reach significance ($p = 0.38$)[32].

Translation of far cortical locking into clinical applications will require site-specific adaptation of far cortical locking design parameters to achieve the desirable amount of motion at the fracture site. In far cortical locking constructs, interfragmentary motion depends on the applied load and on the diameter and length of the far cortical locking screw shaft. Furthermore, motion depends on the number of far cortical locking screws applied on both sides of a fracture as tested in the ovine model. Alternatively, far cortical locking screws may be applied to only one side of a fracture, as is required with periarticular plating where far cortical locking fixation is feasible only in the diaphyseal segment. While these parameters support scalability of far cortical locking constructs to a range of applications, further bench-top studies will be important to document proper scaling of far cortical locking constructs for site-specific applications. In addition to proper scaling, far cortical locking screws require accurate application to obtain a desired motion envelope in the near cortex. If a far cortical locking screw is in contact with the near cortex on insertion, it may reduce or prevent elastic flexion of the screw shafts and thereby may impede reduction of construct stiffness. However, in the current study, despite the use of prototype implants and instrumentation, far cortical locking screws permitted sufficiently accurate application to achieve a greater than sixfold stiffness reduction over a 0.6-mm motion envelope.

The present study has several limitations. First, the number of animals was small; however, the effects of construct stiffness and interfragmentary motion on fracture-healing reached significance despite the small numbers. Second, the stiffness of the fixation constructs was controlled, but interfragmentary motion at the osteotomy gap was dependent on load-bearing by the animal. However, there was no perceptible difference in activity level between the sheep in the far cortical locking and locked plating groups. Third, these results are specific for a 3-mm-gap osteotomy in the ovine tibia and therefore require careful interpretation before extrapolation to the clinical practice. The ovine tibial osteotomy model was selected as it represents the most established fracture-healing model in large animals[18,19]. Load transmission in the ovine tibia has been well characterized and corresponds in magnitude to lower-extremity loading in humans[33,34]. Also, secondary bone healing in sheep is similar to the regeneration process in human bone[35]. Nevertheless, the finding of improved fracture-healing with far cortical locking constructs remains to be confirmed in future clinical studies. Fourth, because of the destructive nature of strength tests, strength assessment was limited to torsion. Torsion was chosen over bending, since bending strength is highly affected by the rotational orientation of the tibia while torsional strength is not[10]. Therefore, torsion results provide a unique summary index for mechanical characterization of the healed tibiae, albeit torsion may not represent the principal loading mode in vivo. Fifth, the torsional results of healed tibiae were not formally compared with those of the intact, contralateral tibiae since only six of the twelve contralateral tibiae had been harvested. As a point of reference, these six intact tibiae had an average torsional strength of 66 ± 8 Nm, and were 2.4 and 1.5 times stronger than the locked plating and far cortical locking specimens, respectively. The intact tibiae had an average energy to failure of 531 ± 119 Nm°, which was 4.8 and 1.9 times higher than that of the locked plating and far cortical locking specimens, respectively. Finally, results are based on implants made of titanium alloy, which is approximately twice as flexible as stainless steel. Hence, locked plating constructs of the same geometry made of stainless steel would permit less interfragmentary motion and could lead to further suppression of callus formation[32].

In conclusion, the results of this study confirmed that callus formation and fracture-healing is dependent on the amount of interfragmentary motion permitted by a locked bridge plating construct. The findings of inconsistent and asymmetric callus formation with locked plating constructs are likely due to their high stiffness and the asymmetric gap closure that attenuates interfragmentary motion toward the cortex adjacent to the plate. The far cortical locking constructs delivered nearly parallel interfragmentary motion of sufficient magnitude to reliably stimulate callus formation around the entire cortex. Because the far cortical locking constructs formed more callus and yielded more consistent and stronger fracture-healing than locked plating constructs, far cortical locking fixation may be advisable to reduce the considerable stiffness of locked bridge plating constructs. However, clinical studies will be required to confirm whether far cortical locking can improve fracture-healing and outcomes of locked plating osteosynthesis in patients.

Appendix

eA A description of stiffness characterization of locked plating and far cortical locking constructs and a figure showing the corresponding test setup and stiffness results are available with the electronic version of this article on our web

site at jbjs.org (go to the article citation and click on "Supporting Data"). ■

NOTE: The authors thank Professor Lutz Claes of the Institute of Orthopaedic Research and Biomechanics in Ulm, Germany, for his advice on study design. The authors thank Trevor Lujan, PhD, and Dan Phelan of the Legacy Biomechanics Laboratory for their contributions to the study preparation and radiographic analysis.

Michael Bottlang, PhD
Josef Doornink, MS
Daniel C. Fitzpatrick, MD
Steven M. Madey, MD
Legacy Biomechanics Laboratory, 1225 N.E.
2nd Avenue, Portland, OR 97232.
E-mail address for M. Bottlang: mbottlan@lhs.org

Maren Lesser, DVM
Brigitte von Rechenberg, DVM, ECVS
Equine Department, Musculoskeletal Research Unit,
Vetsuisse Faculty, University of Zürich,
Winterthurerstrasse 260,
CH 8057, Zürich, Switzerland

Julia Koerber, MS
Peter Augat, PhD
Institute of Biomechanics,
Prof. Kuentscher Strasse 8,
82418 Murnau, Germany

J. Lawrence Marsh, MD
University of Iowa Hospitals and Clinics,
200 Hawkins Drive,
Iowa City, IA 52242

References

1. Fitzpatrick DC, Doornink J, Madey SM, Bottlang M. Relative stability of conventional and locked plating fixation in a model of the osteoporotic femoral diaphysis. Clin Biomech (Bristol, Avon). 2009;24:203-9.

2. Kubiak EN, Fulkerson E, Strauss E, Egol KA. The evolution of locked plates. J Bone Joint Surg Am. 2006;88 Suppl 4:189-200.

3. Ring D, Kloen P, Kadzielski J, Helfet D, Jupiter JB. Locking compression plates for osteoporotic nonunions of the diaphyseal humerus. Clin Orthop Relat Res. 2004;425:50-4.

4. Perren SM. Evolution of the internal fixation of long bone fractures. The scientific basis of biological internal fixation: choosing a new balance between stability and biology. J Bone Joint Surg Br. 2002;84:1093-110.

5. Tan SL, Balogh ZJ. Indications and limitations of locked plating. Injury. 2009;40:683-91.

6. Egol KA, Kubiak EN, Fulkerson E, Kummer FJ, Koval KJ. Biomechanics of locked plates and screws. J Orthop Trauma. 2004;18:488-93.

7. Perren SM. Backgrounds of the technology of internal fixators. Injury. 2003;34 Suppl 2:B1-3.

8. Henderson CE, Bottlang M, Marsh JL, Fitzpatrick DC, Madey SM. Does locked plating of periprosthetic supracondylar femur fractures promote bone healing by callus formation? Two cases with opposite outcomes. Iowa Orthop J. 2008;28:73-6.

9. Uhthoff HK, Poitras P, Backman DS. Internal plate fixation of fractures: short history and recent developments. J Orthop Sci. 2006;11:118-26.

10. Augat P, Penzkofer R, Nolte A, Maier M, Panzer S, v Oldenburg G, Pueschl K, Simon U, Bühren V. Interfragmentary movement in diaphyseal tibia fractures fixed with locked intramedullary nails. J Orthop Trauma. 2008;22:30-6.

11. Claes LE, Heigele CA, Neidlinger-Wilke C, Kaspar D, Seidl W, Margevicius KJ, Augat P. Effects of mechanical factors on the fracture healing process. Clin Orthop Relat Res. 1998;355 Suppl:S132-47.

12. Claes LE, Wilke HJ, Augat P, Rübenacker S, Margevicius KJ. Effect of dynamization on gap healing of diaphyseal fractures under external fixation. Clin Biomech (Bristol, Avon). 1995;10:227-34.

13. Hente R, Füchtmeier B, Schlegel U, Ernstberger A, Perren SM. The influence of cyclic compression and distraction on the healing of experimental tibial fractures. J Orthop Res. 2004;22:709-15.

14. Rahn BA, Gallinaro P, Baltensperger A, Perren SM. Primary bone healing. An experimental study in the rabbit. J Bone Joint Surg Am. 1971;53:783-6.

15. Strauss EJ, Schwarzkopf R, Kummer F, Egol KA. The current status of locked plating: the good, the bad, and the ugly. J Orthop Trauma. 2008;22:479-86.

16. Peindl RD, Zura RD, Vincent A, Coley ER, Bosse MJ, Sims SH. Unstable proximal extraarticular tibia fractures: a biomechanical evaluation of four methods of fixation. J Orthop Trauma. 2004;18:540-5.

17. Bottlang M, Doornink J, Fitzpatrick DC, Madey SM. Far cortical locking can reduce stiffness of locked plating constructs while retaining construct strength. J Bone Joint Surg Am. 2009;91:1985-94.

18. Nunamaker DM. Experimental models of fracture repair. Clin Orthop Relat Res. 1998;355 Suppl:S56-65.

19. Auer JA, Goodship A, Arnoczky S, Pearce S, Price J, Claes L, von Rechenberg B, Hofmann-Amtenbrinck M, Schneider E, Müller-Terpitz R, Thiele F, Rippe KP, Grainger DW. Refining animal models in fracture research: seeking consensus in optimising both animal welfare and scientific validity for appropriate biomedical use. BMC Musculoskelet Disord. 2007;8:72.

20. Epari DR, Kassi JP, Schell H, Duda GN. Timely fracture-healing requires optimization of axial fixation stability. J Bone Joint Surg Am. 2007;89:1575-85.

21. Claes L, Augat P, Suger G, Wilke HJ. Influence of size and stability of the osteotomy gap on the success of fracture healing. J Orthop Res. 1997;15:577-84.

22. Bishop NE, van Rhijn M, Tami I, Corveleijn R, Schneider E, Ito K. Shear does not necessarily inhibit bone healing. Clin Orthop Relat Res. 2006;443:307-14.

23. Lill CA, Hesseln J, Schlegel U, Eckhardt C, Goldhahn J, Schneider E. Biomechanical evaluation of healing in a non-critical defect in a large animal model of osteoporosis. J Orthop Res. 2003;21:836-42.

24. Lujan TJ, Madey SM, Fitzpatrick DC, Byrd GD, Sanderson JM, Bottlang M. A computational technique to measure fracture callus in radiographs. J Biomech. 2010;43:792-5.

25. Augat P, Merk J, Genant HK, Claes L. Quantitative assessment of experimental fracture repair by peripheral computed tomography. Calcif Tissue Int. 1997;60:194-9.

26. Cheal EJ, Mansmann KA, DiGioia AM 3rd, Hayes WC, Perren SM. Role of interfragmentary strain in fracture healing: ovine model of a healing osteotomy. J Orthop Res. 1991;9:131-42.

27. Stoffel K, Dieter U, Stachowiak G, Gächter A, Kuster MS. Biomechanical testing of the LCP—how can stability in locked internal fixators be controlled? Injury. 2003;34 Suppl 2:B11-9.

28. Field JR, Törnkvist H, Hearn TC, Sumner-Smith G, Woodside TD. The influence of screw omission on construction stiffness and bone surface strain in the application of bone plates to cadaveric bone. Injury. 1999;30:591-8.

29. Caja V, Kim W, Larsson S, E YC. Comparison of the mechanical performance of three types of external fixators: linear, circular and hybrid. Clin Biomech (Bristol, Avon). 1995;10:401-6.

30. Foux A, Yeadon AJ, Uhthoff HK. Improved fracture healing with less rigid plates. A biomechanical study in dogs. Clin Orthop Relat Res. 1997;339:232-45.

31. Panagiotopoulos E, Fortis AP, Lambiris E, Kostopoulos V. Rigid or sliding plate. A mechanical evaluation of osteotomy fixation in sheep. Clin Orthop Relat Res. 1999;358:244-9.

32. Seligson D, Mehta S, Mishra AK, FitzGerald TJ, Castleman DW, James AH, Voor MJ, Been J, Nawab A. In vivo study of stainless steel and Ti-13Nb-13Zr bone plates in a sheep model. Clin Orthop Relat Res. 1997;343:213-23.

33. Duda GN, Eckert-Hübner K, Sokiranski R, Kreutner A, Miller R, Claes L. Analysis of inter-fragmentary movement as a function of musculoskeletal loading conditions in sheep. J Biomech. 1998;31:201-10.

34. Taylor WR, Ehrig RM, Heller MO, Schell H, Seebeck P, Duda GN. Tibio-femoral joint contact forces in sheep. J Biomech. 2006;39:791-8.

35. Goodship AE, Watkins PE, Rigby HS, Kenwright J. The role of fixator frame stiffness in the control of fracture healing. An experimental study. J Biomech. 1993;26:1027-35.